

ANALIZA VPLIVA UPORABE POPRAVKOV UR SATELITOV PRI UPORABI METODE PRECISE POINT POSITIONING (PPP)

HIGH RATE 30 SECONDS VS CLOCK INTERPOLATION IN PRECISE POINT POSITIONING (PPP)

Sorin Nistor, Aurelian Stelian Buda

UDK: 52-323.8
 Klasifikacija prispevka po COBISS.SI: 1.04
 Prispelo: 10. 06. 2016
 Sprejeto: 15. 09. 2016

DOI: 10.15292/geodetski-vestnik.2016.03.483-494
 PROFESSIONAL ARTICLE
 Received: 10. 06. 2016
 Accepted: 15. 09. 2016

IZVLEČEK

Razvoj tehnologije GNSS (angl. Global Navigation Satellite Systems), vključno s tehnologijo GPS (angl. Global Positioning System), ter vse večja natančnost in točnost produktov službe IGS (angl. International GNSS Service) prispevajo k vse večji uporabnosti in razširjenosti metode PPP (angl. precise point positioning) za določanje položaja. Služba IGS ponuja popravke o urah satelitov za 30-sekundni interval. V članku obravnavamo in primerjamo rezultate statične določitve položaja z metodo PPP za 30-sekundne popravke ur satelitov in za interpolirane vrednosti 300-sekundnih popravkov ur satelitov. Analiza je izvedena v treh korakih: v prvem je analiziran vpliv obeh vrst popravkov ur na popravke faznih in kodnih opazovanj; v drugem vpliv na makro komponento troposferske refrakcije WTD (angl. wet troposphere delays); v tretjem pa je predstavljena spremenljivost koordinat v smeri vseh treh koordinatnih osi (n , e , h). V raziskavo sta bili vključeni dve postaji IGS, BUCU in SOFI, ter dve postaji EUREF, COST in AUT1. Rezultati kažejo na 30-odstotno povečanje popravkov faznih opazovanj ob uporabi interpoliranih vrednosti 300-sekundnih popravkov ur satelita. Na vrednost mokre komponente troposferske refrakcije WTD znaša razlika do nekaj centimetrov, razlika v koordinatah pa je bila največja v smeri komponente n , in sicer na postaji COST in je znašala 5,79 milimetra.

KLJUČNE BESEDE

GPS, GNSS, PPP, IGS, parametri tirnice, parametri ure satelita

ABSTRACT

The development of GNSS technology (Global Navigation Satellite Systems), including GPS technology (Global Positioning System), and the increase of accuracy and precision of the International GNSS Service (IGS) products, make Precise Point Positioning (PPP) technique more and more attractive. The IGS service provides clock products even for high rate determination – 30 seconds. The article is analyzing and comparing the 30 seconds high rate data and the interpolated data from 300 seconds in static PPP determination. Three stages of analysis are done: in the first stage the impact of data products on LC and PC postfit residuals are accounted, in the second stage the impact on wet troposphere delays (WTD) is analyzed and in the third stage the coordinate variation on North, East and Up component is presented. The stations that were analyzed are two IGS stations, BUCU and SOFI and two EUREF stations: COST and AUT1. The results presented an increase of 30% for LC postfit residuals in the case of interpolated data and no obvious influence on PC postfit residuals. In the case of WTD only a difference of a few centimeters were determined and in the case of coordinate variation the largest difference was present in the North component for station COST of 5.79 mm.

KEY WORDS

GPS, GNSS, PPP, IGS, precise orbit and clock

1 INTRODUCTION

Precise Point Positioning (PPP) method is one of the techniques that is able to determine the coordinates of different points, parameters such as receiver clock error, neutral atmospheric delay, by using the Global Positioning System (GPS). This technique is called precise because it is using precise *a priori* information such as satellite orbits and clock errors, thus resulting in precise and accurate coordinates of the point. The PPP method can be used in a variety of tasks such as geodynamics (Nistor and Buda, 2016a; Amiri-Simkooei, 2009; Yavasoglu et al., 2005; Nistor and Buda, 2016b) tropospheric delay (Nistor and Buda, 2015a; Bevis et al., 1994; Notarpietro et al., 2012), determination of the coordinates of a permanent GPS station (Nistor and Buda, 2015b). The Geodetic Survey Division (GSD) of Natural Resources Canada (NRCan) has used precise orbits and clock products since 1992 for PPP processing (Héroux and Caissy, 1993). With the help of the International GNSS Service (IGS), precise satellite orbit and clock products are available for free which helped the development of the Precise Point Positioning (PPP) technique. The PPP technique is using the data from a single GPS dual frequency receiver – pseudorange and carrier phase observation – and with the help of the IGS products, millimeters accuracy can be achieved. This is possible because of the precise estimated satellite clock and ephemeris (Héroux and Kouba, 2001). The data from IGS service are provided in the following types: Final, Rapid and Ultra-Rapid. The Final orbits from IGS are available with a latency of 12-18 days, the Rapid orbits are between 17-41 hours latency and the Ultra-Rapid are in real-time with half predicted and from 3 to 9 hours for the observed half. The Final orbits and clock are the most accurate data available. The data has been improved over the years from about 30 cm to ~ 2.5 cm precision level for orbits and ~75 ps for clock with a standard deviation of ~ 20 ps. What is interesting is that the Rapid data products present the same accuracy as the Final data products with less tracking station and a faster delivery time. Because the PPP technique can be used in RTK mode, the necessity of the high rate data is recommended and thus contributed to the appearance of the 30s clock products. Due to the short-term variation, satellite clock correction is recommended to be updated very frequently (Bock et al., 2009) which allows to generate high-rate clock corrections within reasonably short time. The problem that is arising is that, a large number of ambiguities that have to be estimated in high rate clock data makes the process quite time consuming (Chen et al., 2014). The orbits do not have to be high rate, because the orbit presents rather small errors which can be absorbed by the estimated clock and this is why even predicted orbits can fulfill the PPP requirements (Chen et al., 2014). In general the estimated satellite clock is done using the undifferenced phase and range observation from a global network.

The PPP technique (Zumberge et al., 1997; Héroux and Kouba, 2001) represents a pragmatic instrument that it is able to reduce significant the computation burden for application where the co-variance among parameters are not of interest for different stations. An important issue of the PPP determination is the ambiguity fixing which can reduce the time convergence, an improve the accuracy of PPP significantly (Ge et al., 2008; Laurichesse et al., 2009; Geng et al., 2010). Due to the fact that the narrow-lane ambiguity has a wavelength of only 10 cm, the short-term clock accuracy should be better than 3 cm for fast and reliable ambiguity fixing, although the estimation process can be accelerated by epoch-differenced observations (Ge et al., 2008; Ge et al., 2009; Zhang et al., 2007). One of the most important problems in PPP ambiguity fixing is the zero-difference (ZD) ambiguity of a

satellite-receiver pair or the single-difference (SD) ambiguity which is not an integer value because of the uncalibrated phase delays (UPD) originating in the satellite and receiver (Blewitt, 1989). In double difference, the ambiguity (DD) can be relatively easy to fix, because the UPDs is canceled. Combining PPP solutions of simultaneously observed stations, ambiguities for DD can be defined and fixed in the same way as for network solutions (Zumberge et al., 1997; Blewitt et al., 2005). In a global network more than 97% of the DD ambiguities are resolved to integer value by optimization of the selection and the rate of fixing is slightly correlated with the baseline length, which implies that fractional parts of the two SD ambiguities, which makes the DD ambiguity, must be in consent with each other very well (Ge et al., 2005). If this condition is not met, their difference would not be close to an integer (Ge et al., 2008).

2 MATERIALS AND METHODS

The ionospheric-free combination of GPS pseudorange (PC) and the carrier-phase observation (LC) are related to the user position, troposphere delay, clock and ambiguity parameters according to the simplified observation equations (H eroux and Kouba, 2001):

$$PC = \rho + c(dt - dT) + T_r + \varepsilon_p \tag{1}$$

$$LC = \rho + c(dT - dt) + T_r + N\lambda + \varepsilon_\phi \tag{2}$$

where:

- PC is the ionosphere-free combination of P1 and P2 pseudoranges ($2.54 P_1 - 1.546 P_2$),
- LC is the ionosphere-free combination of L1 and L2 carrier-phases ($2.54\lambda_1 \Phi_1 - 1.546\lambda_2 \Phi_2$),
- dT is the station receiver clock offset from the GPS time,
- c is the vacuum speed of light,
- dt is the satellite clock offset from the GPS time,
- T_r is the signal path delay due to the neutral-atmosphere (primarily the troposphere),
- N is the non-integer ambiguity of the carrier-phase ionosphere-free combination,
- $\lambda_1, \lambda_2, \lambda$ are the carrier- phase L1, L2 and combination (10.7 cm) wavelengths, respectively,
- $\varepsilon_p, \varepsilon_\phi$ are the relevant measurement noise components, including multipath.

The argument ρ represents the geometrical range computed by iteration from the satellite position (X_s, Y_s, Z_s) at the transmission epoch and the station position (x, y, z) at the reception epoch $T = t + \rho / c$:

$$\rho = \sqrt{(X_s - x)^2 + (Y_s - y)^2 + (Z_s - z)^2} \tag{3}$$

In the case of relative positioning between the two stations (i, j) the satellite clock errors tend to be eliminated simply by subtracting the corresponding observation equations (1), (2) made by the two stations (i, j) to the same satellite (k) (H eroux and Kouba, 2001) :

$$PC_{ij}^k = \Delta\rho_{ij}^k + c\Delta dT_{ij} + \Delta T_{rij}^k + \Delta\varepsilon_{Pij}^k \tag{4}$$

$$LC_{ij}^k = \Delta\rho_{ij}^k + c\Delta dT_{ij} + \Delta T_{rij}^k + \Delta N_{ij}^k \lambda + \Delta\varepsilon_{Lij}^k \tag{5}$$

In the equations (4) and (5), $\Delta(\rho)_{ij}^k$ represents the single difference. By subtracting the observation equations (4), (5) towards to stations (i, j) and the satellite (k) from the corresponding equations of the stations

(i, j) to the satellite, the so called double differenced observation equations can be formed, in which the station clock difference errors is the same for both single differences, is eliminated:

$$PC_{ij}^{kl} = \Delta\rho_{ij}^{kl} + \Delta T_{rij}^{kl} + \Delta\varepsilon_{p_{ij}}^{kl} \quad (6)$$

$$LC_{ij}^{kl} = \Delta\rho_{ij}^{kl} + \Delta T_{rij}^{kl} + \Delta N_{ij}^{kl} \lambda + \Delta\varepsilon_{L_{ij}}^{kl} \quad (7)$$

In this equations $\Delta(\rho)_{ij}^{kl}$ represents the double difference for the (i, j) station and (k, l) satellite pairs. Additionally, the initial L1 and L2 phase ambiguities that are employed to evaluate the ionospheric-free ambiguities ΔN_{ij}^{kl} become integers. This is resulting by the fact that fractional phase initializations on L1 and L2 for the (i, j) station and (k, l) satellite pairs, much like station/satellite clock errors, are also eliminated by the above double differencing scheme. If the L1 and L2 ambiguities are resolved to integers, the ionospheric-free ambiguities ΔN_{ij}^{kl} also become known and thus can be eliminated from the equation (7), which is equivalent to the equation for pseudorange (6) - double differenced phase observations with integer ambiguity become precise pseudorange observations that result from unambiguous precise phase measurement differences. This implies that fixed ambiguity in relative positioning yields the highest accuracy and precision for GPS measurements.

The equations (1), (2), (6) and (7) appear to be quite different, due to a different number of unknowns and individual terms with different magnitudes. For example the un-differenced tropospheric delay ΔT_r is much higher than the double differenced tropospheric delay ΔT_{rij}^{kl} , the noise $\Delta\varepsilon_{p_{ij}}^{kl}$ and $\Delta\varepsilon_{L_{ij}}^{kl}$ is much larger than the original un-differenced noise $\Delta\varepsilon_p$ and $\Delta\varepsilon_L$. Double differenced and un-differenced approaches produce the same results, provided by the same set of un-differenced observations and proper correlation, which is derived by using the differencing technique. This can be explained as such: the un-correlated, un-differenced solutions where the (satellite/station) clock unknowns are solved for each observation epoch is completely equivalent to the position solutions resulted by using the double difference technique (Kouba, 2009).

The article is using the PPP technique in which the IGS precise orbit and clock are used, in equation (1) and (2) the satellite clock (dt) is considered fixed (the values are known) and thus it can be removed. In addition, the tropospheric path delay (T_r) as a product of the zenith path delay (zpd) and mapping function (M) which relates slant path delay to (zpd) and thus the mathematical model for point positioning is (Kouba, 2009):

$$PC_{PPP} = \rho + cdT + Mzpd + \varepsilon_p - PC = 0 \quad (8)$$

$$LC_{PPP} = \rho + dT + Mzpd + N\lambda + \varepsilon_\phi - LC = 0 \quad (9)$$

The equations (8) and (9) after fixing the satellite position and clock (they are considered known) contain observations and unknowns pertaining only to a single station unlike the equations (1)-(7) that contain unknowns and/or observation differences involving baselines or the whole station network. It can be seen that the satellite clock and orbit weighting does not require satellite clock and position parameterizations, because the satellite position and clock can be very well accounted by the specific satellite pseudorange/phase observation weighting and thus result that it is unnecessary to solve equation (8) and (9) in a network solution due to the fact that will results in uncorrelated station solutions which is exactly identical to the independent solutions from the point positioning estimation of a single station.

3 PROCESSING AND RESULTS

The article is presenting the effects on LC, PC postfit residuals, the zenith tropospheric delay and the coordinates shift of four permanent GPS stations by using in the first stage of the estimation the high rate 30 seconds precise clock information and then by using the 300 seconds clock information which is interpolated by using the third polynomial order for estimating the data at 30 seconds. The precise ephemeris and clock information from final products was used and they have been downloaded from Jet Propulsion Laboratory (JPL) site. The software that is used for presenting the effect of the clock on PPP determination is Gipsy-Oasis from JPL (Zumberge et al., 1997).

The process data are from station BUCU, COST stations that are from Romania, AUT1 which is a station from Greece and SOFI which is a station from Bulgaria. The RINEX data contains 24 hours of GPS measurements and the processing was done on static mode. The station BUCU and SOFI are IGS stations and station COST and AUT1 are EUREF stations. Stations BUCU and COST are also integrated in Romanian Position Determination System (ROMPOS). The settings for processing data RINEX files were the same for all stations in which the minimum elevation cutoff was set to 15°, the data weight for LC was 1 cm and for PC 1 m and the method for elevation dependent weighting was set for $\sqrt{(\sin(\text{elevation}))} / \text{sigma}$. For the zenith tropospheric delay a random walk value of $5.0 \cdot 10^{-8} \text{ km} / \sqrt{\text{sec}}$ was applied and for horizontal delay gradients a random walk value of $5.0 \cdot 10^{-9}$. The tropospheric mapping function was VMF1 (Boehm et al., 2006). The interval for processing was set to 30 seconds.

In the first stage of the estimation 30-second high rate clock was used for all stations. In the next part of the estimation 300 seconds interval was interpolated to process the data at 30 seconds. The results for LC postfit residuals are presented in Figure 1.

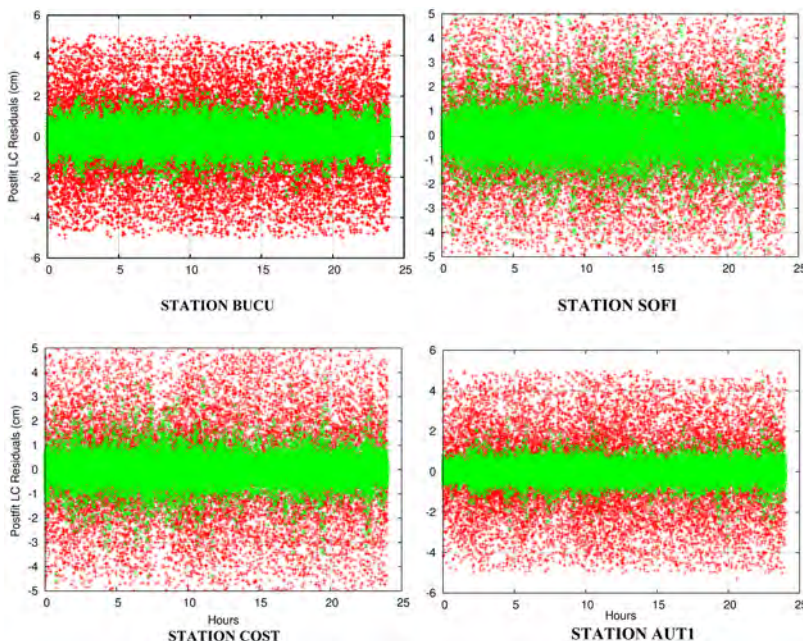


Figure 1: LC postfit residuals: in the upper part are the IGS stations: BUCU and SOFI; in the lower part are the EUREF stations COST and AUT1.

The results for stations BUCU and SOFI which are IGS stations, in terms of LC postfit residuals, are presented in the upper part of the plot, left side respectively the right side and the lower part of the plot present the results for the two EUREF stations COST and AUT1, where the first is presented in the left side and the second, in the right side. The points (bright crosslets) represent the LC postfit residuals after estimation using the 30 seconds high rate clock data from JPL. The red points (dark crosslets) represent the LC postfit residuals after processing the data using the 300 seconds clock data which have been interpolated. The LC postfit residuals for station BUCU when the 30 seconds high rate clock data is used, is significant smaller than in the case of interpolated clock data. They present an approximate constant behavior on the entire 24-hours period. The postfit residuals for LC in the case that the 30 seconds high rate clock data is used, is 5.60 mm for a 21078 number of points. In this case no outlier was detected. It can be seen that the scatter is between ± 12 mm. The postfit residuals for LC in the case that the 300 seconds were interpolated, the result is 18.660 mm. In this case a number of 1607 outliers were detected and the scatter varies between ± 40 mm. In the case of the other IGS station – station SOFI, by using the 30-second high rate data the LC postfit residuals presented a value of 8.49 mm, but a number of 43 outliers were present in the solutions, which can be attributed to the increase of the postfit residuals for LC solution. If the interpolated clock data was used, a number of 1722 outliers were present in the solutions which generated a postfit residual of 19.04 mm for LC combination. In the case of station COST when the 30 seconds high rate clock data is used, the LC postfit residuals is 5.91 mm. There is a slight increase compared to the data from station BUCU. This increase can be attributed to the fact that in the estimation process by using the same setting as in the previous case, a number of two outliers were detected. The postfit residuals for LC in the case that the 300 seconds were interpolated, the result is 18.631 mm. By using the interpolated data clock the number of outliers increased to a total number of 1686. For EUREF station AUT1 when the high rate 30 second clock data was used, the LC postfit residual presented a value of 4.31 mm and no outlier were present in the solution. When the interpolated clock data was used, the LC postfit residual were 18.45 mm and a number of 1589 outlier were present in the solution.

In the case of PC postfit residuals the results are presented in Figure 2.

The results for stations BUCU and SOFI in terms of PC postfit residuals are presented in the upper part of the plot, first in the left side respectively the right side and the lower part present the results for station COST in the left side and in the right side the results for station AUT1. The green points (bright crosslets) represent the PC postfit residuals after estimation using the 30 seconds high rate clock data from JPL. The red points (sharp crosslets) represent the PC postfit residuals after processing the data using the 300 seconds clock data which have been interpolated. From the plot we can observe that all stations – BUCU, SOFI, COST and AUT1 – don't present noticeable differences between the 30 seconds high rate clock and the interpolated 300 second data. In the case of station BUCU the PC postfit residuals were 65.85 cm and 65.94 cm for the interpolated data. No outliers were detected. The station SOFI presented a value 79.39 cm when the high rate data was used and 79.42 cm in the case of interpolated data. For station COST the PC postfit residuals were 64.20 cm and 64.25 in the case of the interpolated clock data. For this station the PC presented in both case one outlier. The station AUT1 presented a value of 58.78 cm in the case of high rate data and 59.01 cm in the case of interpolated data for PC postfit residuals. In this station in the last hour it can be observed that the data presented a bias of 100 cm. In this station no outliers were determined in the solution for PC.

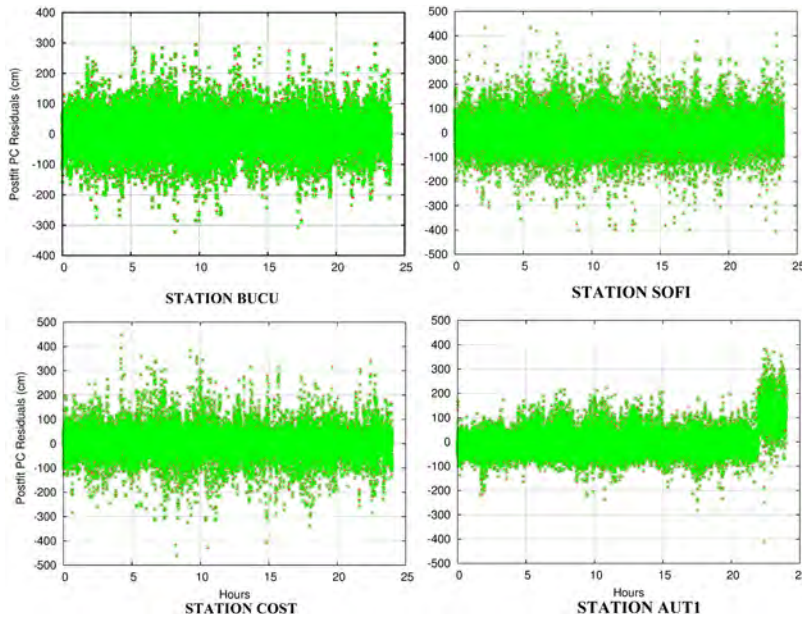


Figure 2: PC postfit residuals: in the upper part are the IGS stations BUCU and SOFI and in the lower part are the EUREF stations COST and AUT1.

In the next part of the analysis it is presented the impact of 30 seconds high rate clock data and the 300 seconds interpolated clock data on wet tropospheric delay (WTD) which is presented in Figure 3.

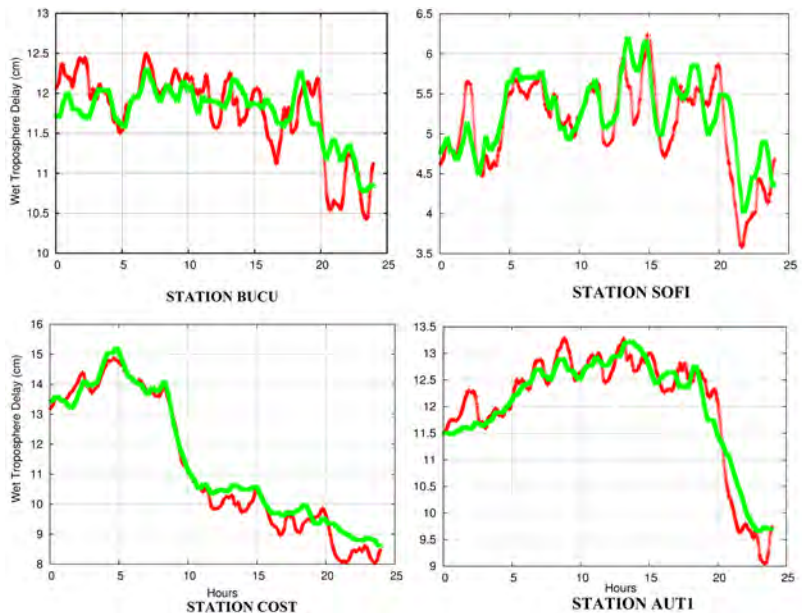


Figure 3: Wet tropospheric delay: in the upper plot are the IGS stations BUCU and SOFI and in the lower plot are the EUREF stations COST and AUT1.

The results for IGS stations BUCU and SOFI in terms of wet tropospheric delay is presented in the left respectively right side of the upper plot and the lower part of the plot present the results for station COST in the left side and in the right side is the AUT1 station. The green (bright) line represents the wet tropospheric delay when the 30 seconds high rate clock data from JPL was used in the estimation process. The red (dark) line represents the wet tropospheric delay after processing the data using the 300 seconds clock data which have been interpolated. For the station BUCU we can observe from the plot that there is a large variation between the 30 seconds high rate clock – first case - and the interpolated data – second case. The WTD in the first case starts at a value of 11.73 cm where in the second case the WTD starts at 12.06 cm, a difference of 0.33 cm. The smallest value of WTD in the first case was around 23.35 hours from the beginning with a value of 10.77 cm with a sigma of 1.49 mm, where in the second case the smallest value was around 23.4 hours from the beginning but with a value of 10.429 cm with a sigma of 1.55 mm. The highest value of WTD when the 30 seconds high rate clock data was used, was obtained around 7.25 hours from the beginning with a value of 12.306 cm and a sigma of 1.31 mm, where in the case of interpolated data the highest value was obtained around 7.20 hours from the beginning with a value of 15.201 cm and a sigma of 1.35 mm. Although there is a different variation of WTD in the case of 30 seconds high rate clock data and the interpolated data, the highest and lower value of WTD were obtained about the same hour of the day. The largest difference between the two determinations was around 20.55 hours with a value of 0.93 cm. Also in terms of precision both methods presents a maximum sigma of 2 mm for station BUCU. For station SOFI in the case of high rate data the starting value was 4.758 cm and in the case of interpolated data the WTD started at 4.608 cm, a difference of 0.15 cm. The sigma in the first case was 2.4 mm and in the second case 2.5 mm. In the case of station SOFI the WTD is presenting almost the same pattern, the lowest value was encountered at the same time – 22.15 hours from the beginning. In the case of station COST no noticeable variation of WTD can be observed between the 30 seconds high rate clock and the interpolated data. The WTD in the first case starts at a value of 13.42 cm where in the second case the WTD starts at 13.18 cm, a difference of 0.24 cm. The smallest value of WTD in the first case was around 23.35 hours from the beginning with a value of 8.61 cm and a sigma of 2.02 mm, where in the second case the smallest value was around 23.30 hours from the beginning but with a value of 8.02 cm with a sigma of 1.72 mm. The highest value of WTD for the 30 seconds high rate clock data, was obtained around 4.4 hours from the beginning with a value of 15.20 cm and a sigma of 1.24 mm, where in the case of interpolated data the highest value was obtained around 4.30 hours from the beginning with a value of 14.866 cm and a sigma of 1.32 mm. It can be observed also that in the station COST not only the highest and lowest value of WTD appears on the same period, but also their trends are almost the same on the entire 24-hour period. For station AUT1 it seems that in the case of high rate data presents a smoother behavior that in the case of the interpolated data where we can see very drastic changes of the values for the entire period, where in the case of high rate data the changes are smaller – they don't present peaks. This station is the only case when both methods starts the WTD at almost the same value – the difference between the two cases was 0.02 cm and is ending at almost the same value – a difference of 0.04 cm.

The variation of coordinates related to stations BUCU, SOFI, COST and AUT1 by using the 30 seconds high rate clock data and 300 seconds clock data which have been interpolated, are presented in Figure 4.

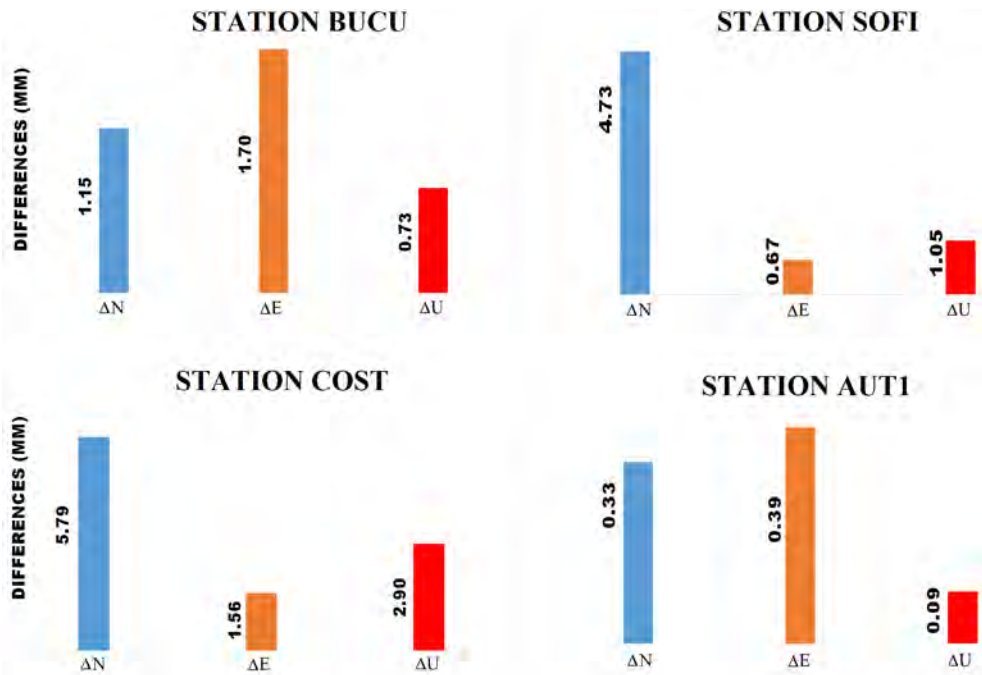


Figure 4: Coordinates variation: the IGS stations BUCU and SOFI are in the upper part of the plot and the EUREF stations COST and AUT1 in the lower part of the plot.

The blue bar from the plot represents the difference on North component between the value that was estimated by using the 30 seconds high rate clock – first case - and the value that resulted by using the 300 seconds clock data which have been interpolated – second case. The orange bar represents the difference on East component between the values that were estimated in the first case and the value that resulted in the second case. The red (dark) bar represents the difference on Up component between the value that was estimated by using the 30 seconds high rate clock and the value that resulted by using the 300 seconds clock data which have been interpolated. The station BUCU for the North component presented a small variation – 1.15 mm, but for the East component presented a higher variation – 1.70 mm and for the Up component only a variation of 0.73 mm was present. The other IGS station, station SOFI presented a higher variation in the North component, a value of 4.73 mm, for the East component the smallest difference was detected, a value of 0.67 mm and for the Up component a difference of 1.05 mm. For station COST the variation is much higher than in the case of station BUCU and SOFI. For the North component the variation presents a magnitude of 5.79 mm, for the East component 1.56 mm and for the Up component a difference of 2.90 mm was present. The smallest difference on all three components were present in the case of station AUT1 with 0.33 mm, 0.39 mm and 0.09 mm.

4 CONCLUSION

The impact of the 30 seconds high rate clock and the interpolated data, on LC, PC postfit residuals, WTD and coordinate shifts was analyzed. In Table 1 the impact of clock data on LC and PC postfit residuals are summarized.

Table 1: Impact of 30-second high rate data clock and interpolated data on LC and PC postfit residuals

Station Name	Clock data			
	30 second		300 second (interpolated data)	
	LC (mm) (postfit residuals)	PC (mm) (postfit residuals)	LC (mm) (postfit residuals)	PC (mm) (postfit residuals)
BUCU	5.60	658.5	18.66	659.4
SOFI	8.49	793.9	19.04	794.2
COST	5.91	642.0	18.63	642.5
AUT1	4.31	587.8	18.45	590.1

In the case of interpolated data, the LC postfit residuals “suffered” an increase of three times excepting station SOFI where the increase was only two times higher. For station BUCU the interpolated clock data generated a number 1607 outliers which represents approximately 8% from the total data. In the case of station SOFI, the number of outliers in the case of interpolated data reached 1722. For station COST and AUT1 the use of interpolated data generated 1686 outliers respectively 1589. It can be seen that the interpolated data generates approximately the same percentage of outliers for all the stations, around 8% from the total data. The impact on PC postfit residuals is not noticeable, but in the case of WTD for station BUCU only for a period of four hours – from three to seven hours from the beginning - the behavior of the values were approximately the same – the largest variation was 0.8 cm. For station SOFI the same behavior was present for a longer period – from three to fifteen hours from the beginning with the highest variation of 0.4 cm. In the case of station COST this behavior maintains also for a long period – from two to eleven hours from the beginning – but also for the rest of the period the variation of the values is relatively small – the largest variation was 1 cm. For station AUT1 the WTD of the high rate data generated a smoothed behavior and the tendency remains the same on the entire period with the WTD reported by using the interpolated data. In Table 2 the impact of clock data on coordinates are summarized.

Table 2: Impact of 30 second high rate data clock and interpolated data on coordinate determination

Station Name	Coordinate differences		
	North (mm)	East (mm)	Up (mm)
BUCU	1.15	1.70	0.73
SOFI	4.73	0.67	1.05
COST	5.79	1.56	2.90
AUT1	0.33	0.39	0.09

Although the difference between 30 seconds high rate clock and interpolated data presented noticeable difference on LC postfit residuals, the difference on North, East and Up components presented relatively small differences. The largest shift was on station COST on the North component of 5.79 mm, which also experienced the largest shift on Up component. Correlating with the results from Table 1, we can observe that the station didn't experience the highest LC postfit residuals in neither of the cases. On the North and Up component the presence of outliers which were detected only on stations SOFI and COST by using the 30-second high rate data clock, generated the largest shift; on East component the station BUCU experienced the largest shift, but no outliers were detected in this station. The smallest

coordinates variation was on station AUT1 which presented also the lowest LC postfit residuals on both high rate and interpolated data. We can conclude that in the stations BUCU and AUT1 were no outliers were detected for LC postfit residuals in the case of high rate data, the variation on all three components presented the smallest values.

Depending on the type of application the use of high rate data clock can be used or not. IGS rapid and final clock products include traditionally clock correction at intervals of 300 seconds. There are now a few Analysis Centers that provide high rate clock products with a sampling of 30 seconds such as Jet Propulsion Laboratory (JPL), Center for Orbit Determination in Europe (CODE) or Massachusetts Institute of Technology (MIT). The clock correction is essential for Precise Point Positioning which can be used in multiple GPS application. To obtain high accuracy results it is recommended to use clock correction which are sampled the same as the GPS observation – in our case 30 seconds. The 300 seconds clock correction can be interpolated but they are not accurate enough to be used in high accurate PPP determination as also shown in (Montenbruck et al., 2005).

Literature and references:

Amiri-Simkooei, A. (2009). Noise in multivariate GPS position time-series. *Journal of Geodesy*, 83 (2), 175–187. DOI: <http://dx.doi.org/10.1007/s00190-008-0251-8>

Bevis, M., Businger, S., Chiswell, S., Herring, T. A., Anthes, R. A., Rocken, C., Ware, R. H. (1994). GPS meteorology: Mapping zenith wet delays onto precipitable water. *Journal of applied meteorology*, 33 (3), 379–386. DOI: [http://dx.doi.org/10.1175/1520-0450\(1994\)033<0379:GMMZWD>2.0.CO;2](http://dx.doi.org/10.1175/1520-0450(1994)033<0379:GMMZWD>2.0.CO;2)

Blewitt, G. (1989). Carrier phase ambiguity resolution for the Global Positioning System applied to geodetic baselines up to 2000 km. *Journal of Geophysical Research: Solid Earth*, 94 (B8), 10187–10203. DOI: <http://dx.doi.org/10.1029/JB094iB08p10187>

Blewitt, G., Hammond, W., Kreemer, C., Plag, H. P. (2005). From Yucca Mountain local stability to global quaking: GPS point positioning strategies spanning the spatio-temporal spectrum. *advances in GPS data processing and modelling for geodynamics*, University College London, 9–10.

Bock, H., Dach, R., Jäggi, A., Beutler, G. (2009). High-rate GPS clock corrections from CODE: support of 1 Hz applications. *Journal of Geodesy*, 83 (11), 1083–1094. DOI: <http://dx.doi.org/10.1007/s00190-009-0326-1>

Boehm, J., Werl, B., Schuh, H. (2006). Troposphere mapping functions for GPS and very long baseline interferometry from European Centre for Medium-Range Weather Forecasts operational analysis data. *Journal of Geophysical Research*, 111 (B2), B02406. DOI: <http://dx.doi.org/10.1029/2005JB003629>

Chen, H., Jiang, W., Ge, M., Wickert, J., Schuh, H. (2014). Efficient High-Rate Satellite Clock Estimation for PPP Ambiguity Resolution Using Carrier-Ranges. *Sensors (Basel, Switzerland)*, 14 (12), 22300–22312. DOI: <http://dx.doi.org/10.3390/s14122300>

Ge, M., Chen, J., Gendt, G. (2009). EPOS-RT: software for real-time GNSS data processing. In: *Geophysical research abstracts*.

Ge, M., Gendt, G., Dick, G., Zhang, F. P. (2005). Improving carrier-phase ambiguity resolution in global GPS network solutions. *Journal of Geodesy*, 79 (1–3), 103–110. DOI: <http://dx.doi.org/10.1007/s00190-005-0447-0>

Ge, M., Gendt, G., Rothacher, M. al, Shi, C., Liu, J. (2008). Resolution of GPS carrier-phase ambiguities in precise point positioning (PPP) with daily observations. *Journal of Geodesy*, 82 (7), 389–399. DOI: <http://dx.doi.org/10.1007/s00190-007-0187-4>

Geng, J., Meng, X., Teferle, F. N., Dodson, A. H. (2010). Performance of precise point positioning with ambiguity resolution for 1-to 4-hour observation periods. *Survey Review*, 42 (316), 155–165. DOI: <http://dx.doi.org/10.1179/003962610X1257516251682>

Héroux, P., Caissy, M. (1993). Canada’s active control system data acquisition and validation. *Geomatica*, 47 (3–4), 233–244.

Héroux, P., Kouba, J. (2001). GPS precise point positioning using IGS orbit products. *Physics and Chemistry of the Earth, Part A: Solid Earth and Geodesy*, 26 (6), 573–578. DOI: [http://dx.doi.org/10.1016/S1464-1895\(01\)00103-X](http://dx.doi.org/10.1016/S1464-1895(01)00103-X)

Kouba, J. (2009). A guide to using International GNSS Service (IGS) products.

Laurichesse, D., Mercier, F., Berthias, J.-P., Broca, P., Cerri, L. (2009). Integer Ambiguity Resolution on Undifferenced GPS Phase Measurements and Its Application to PPP and Satellite Precise Orbit Determination. *Navigation*, 56 (2), 135–149. DOI: <http://dx.doi.org/10.1002/j.2161-4296.2009.tb01750.x>

Montenbruck, O., Gill, E., Kroes, R. (2005). Rapid orbit determination of LEO satellites using IGS clock and ephemeris products. *GPS Solutions*, 9 (3), 226–235. DOI: <http://dx.doi.org/10.1007/s10291-005-0131-0>

Nistor, S., Buda, A. S. (2015a). Using different mapping function in GPS processing for remote sensing the atmosphere. *Journal of Applied Engineering Science*, 5 (2). DOI: <http://dx.doi.org/10.1515/jaes-2015-0024>

Nistor, S., Buda, A. S. (2015b). Ambiguity Resolution In Precise Point Positioning Technique: A Case Study. *Journal of Applied Engineering Sciences*, 5 (1), 53–60. DOI: <http://dx.doi.org/10.1515/jaes-2015-0007>

Nistor, S., Buda, A. S. (2016a). GPS network noise analysis: a case study of data collected over an 18-month period. *Journal of Spatial Science*, 1–14. DOI: <http://dx.doi.org/10.1080/14498596.2016.1138900>

- Nistor, S., Buda, A. S. (2016b). The Influence of Different Types of Noise on the Velocity Uncertainties in GPS Time Series Analysis. *Acta Geodynamica et Geomaterialia*, 13 (4(184)), 387–394. DOI: <http://dx.doi.org/10.13168/AGG.2016.0021>
- Notarpietro, R., Cucca, M., Bonafoni, S. (2012). GNSS Signals: A Powerful Source for Atmosphere and Earth's Surface Monitoring. *Yann Chemin (for InfTech)*. DOI: <http://dx.doi.org/10.5772/33489>
- Yavasoglu, H., Tari, E., Sahin, M., Karaman, H., Erden, T., Bilgi, S., Erdogan, S. (2005). Applications of Global Positioning System (GPS) in geodynamics: with three examples from Turkey. *Proceedings of 2nd International Conference on Recent Advances in Space Technologies*, 2005. RAST 2005. DOI: <http://dx.doi.org/10.1109/RAST.2005.1512597>
- Zhang, Q., Moore, P., Hanley, J., Martin, S. (2007). Auto-BAHN: Software for near real-time GPS orbit and clock computations. *Advances in Space Research*, 39 (10), 1531–1538. DOI: <http://dx.doi.org/10.1016/j.asr.2007.02.062>
- Zumberge, J. F., Heflin, M. B., Jefferson, D. C., Watkins, M. M., Webb, F. H. (1997). Precise point positioning for the efficient and robust analysis of GPS data from large networks. *Journal of Geophysical Research*, 102 (B3), 5005. DOI: <http://dx.doi.org/10.1029/96JB03860>



Nistor S., Buda A. S. (2016). High rate 30 seconds vs clock interpolation in precise point positioning (PPP). *Geodetski vestnik*, 60 (3): 483–494. DOI: 10.15292/geodetski-vestnik.2016.03.483-494

Sorin Nistor, Ph.D.

*University of Oradea, Faculty of Constructions and Architecture
4, Barbu Ștefănescu Delavrancea
410058 Oradea, Romania
e-mail: sonistor@uoradea.ro*

Aurelian Stelian Buda, Ph.D.

*University of Oradea, Faculty of Constructions and Architecture
4, Barbu Ștefănescu Delavrancea
410058 Oradea, Romania
e-mail: budaurelian68@yahoo.ro*